DIRECT MEASUREMENT OF MAMMALIAN AXONEMAL DYNEIN'S MOTOR ACTIVITY

by

David P. Lorch

A dissertation submitted in partial fulfillment
of the requirements for the degree of
Doctor of Philosophy
(Biomedical Engineering)
in The University of Michigan
2010

Doctoral Committee:

Associate Professor Alan J. Hunt, Chair
Professor Edgar Meyhöfer
Associate Professor Shuichi Takayama
Professor Charles B. Lindemann, Oakland University

DEDICATION

There are too many groups, people, & animals to dedicate this thesis to, so I am going to make a list in no particular order:

My pets growing up: Lila, Golda, Sefira, and Malka

Star Trek

My parents, Dr. Steven & Harriet Lorch

My siblings, Dr. Jacob Lorch and Elisa Berger

My niece and nephew, Shayna and Jeffrey Berger

Close friends: Joe Waldman, Amandine Abraham, Anne Adams Bliss, Diana Hilton, Thomas Ambrose, Oliver Yu, Eric Kampe, The Williams Family (Justin, Stephanie, Bridget, Eric), Wayne Fung, Christine Kryscio, Sarah Monje, Dr. Somnath Chowdhury, Devorah Matthews and any others I may be forgetting.

The M Go Blue Bots, WISE, M-STEM, CRLT, The College of Engineering and all of my students from the past 11 years

Susan Bitzer who first put me on a path to a PhD

My labmates, especially Dr. Damon Hoff, Dr. Henry Schek, and Blake Charlebois

Chuck, for repairing my computer when my hard drive fried right before my qualifying exams

ACKNOWLEDGMENTS

I would most like to thank Dr. Damon Hoff, for his help throughout my PhD. He has always been available and incredibly helpful with everything from scientific advice to editing/critiques. Also, most of my work could not have been done without Dr. Henry Schek and Dr. Gary Brouhard first setting up the optical tweezers and the great help and advice that they provided to me as well as senior graduate students. And of course I also want to thank my current and past labmates Blake Charlebois, Jeff Herbstman, Dr. Sanghyun Lee, Dr. Jun Chen, Dr. Kevin Ke, Dr. Ran An, Seth McCubbin, and Dr. Ajit Joglekar for their camaraderie and discussions.

Thank you also to my committee members Dr. Charles Lindemann, Dr. Edgar Meyhöfer, Dr. Shuichi Takayama, and of course my advisor Dr. Alan Hunt. Dr. Hunt was my professor first for BME 418: Quantitative Cell Biology, and was kind enough to let me join his lab and later to discover my desire to teach by being a GSI for his course. I am greatly appreciative to Dr. Lindemann's lab at Oakland University, especially Kathleen Lesich, for help editing, for answering many questions, and preparing experimental samples.

Thank you to the WISE organization, the M Go Blue Bots, and especially Dr. Cinda-Sue Davis, Jamie Saville, and Ruth Lum for letting me be a part of their programs; it was easily the most rewarding time that I've spent in graduate school.

TABLE OF CONTENTS

LIST OF FIGURES

LIST OF TABLES

CHAPTER 2

CHAPTER 3

CHAPTER 1

THE CYTOSKELETON & THE AXONEME

While the focus of this thesis is the protein dynein, it is important conceptually to start at a much higher level with the cell. A cell is made up of both structural and functional components that are crucial to its life. Dynein is a functional component, but interacts with a very important structural component: microtubules (MT). MTs are one of the parts of the cytoskeleton (the "skeleton" of the cell inside of its cytoplasm) providing support to the cell as well as providing roads/tracks that molecular motors such as dynein move along within the cell. MTs are also found in a structure called the axoneme which is inside the tails (cilia/flagella) of cells which allow cells to produce motion around itself or of itself. Dynein in the axoneme traveling along, as well as being attached to, these MTs are what produce these cellular-scale motions. Dynein that use the cytoskeleton are called cytoplasmic dynein and dynein that are contained within the axoneme are called axonemal dynein. The focus in this thesis will be axonemal dynein (specifically in mammals), but discussing cytoplasmic dynein is of the upmost importance for comparison and continuance of research progress.

1.1 Microtubules

MTs are vital to dynein because without them dynein can not produce any productive motion. MTs are long, cylindrical polymeric structures made up of a protein

called tubulin. α–β tubulin dimers are 8 nm in length and string together to form protofilaments. These protofilaments are bound together in parallel in a circle, creating a tubal shape, the MT. For the most part, standard MTs have 13 protofilaments making up this circle though MTs can occur in other numbers (as will be described below in a special case of the doublet microtubule inside of the axoneme).

When a MT polymerizes, tubulin dimers can be added to either end. While both ends allow addition of tubulin, the rate at which tubulin is added helps to define the two ends of the MT. The end referred to as the + (plus) end is the end that tubulin is added to at a faster rate while the – (minus) end has tubulin added at a slower rate. This produces a polarity of MTs which becomes important when discussing what direction along the MT a molecular motor is travelling. This polymerization of MTs with tubulin occurs naturally in the cell, but can also be done *in situ*. This makes it possible to study the motion of molecular motors by isolating the components for study outside of the cell. This polymerization of MTs *in situ* is done throughout the rest of our mammalian, axonemal dynein studies.

1.2 Molecular Motors

Dynein is one of three known types of ATP-dependent motor molecules that have the principal function of generating intracellular forces; the other two are kinesin and myosin. Motor molecules convert chemical energy, Adenosine Triphosphate (ATP), into mechanical movement. Kinesin and myosin are also found along the cytoskeleton of a cell, just like dynein. The main differences between the motors (with respect to travel) is

that myosin is associated with a different cytoskeletal element, actin filaments, instead of MTs. Kinesin uses MTs though it travels in the opposite direction (of the MT) of dynein. Myosin is also more commonly known as the motor molecule that causes the contraction of muscle. Although dynein was first recognized over 40 years ago [Gibbons and Rowe, 1965], relatively little is certain about its basic biochemistry and mechanics. Dyneins can be classified into those involved in intracellular transport (cytoplasmic dynein) and flagellar/ciliary movement (axonemal dynein). Flagella and cilia play critical roles providing propulsion for swimming cells (such as sperm) and moving fluids across tissue surfaces (such as the inner lining of the lungs) in mammals and other eukaryotes. Such dynein-mediated activities are vital to mammalian life.

1.3 Cilia & Flagella

Flagellar/ciliary bending is caused by the sliding of doublet MTs past each other due to dynein motors attached to one doublet MT "walking" along an adjacent doublet MT; this occurs in a structure at the core of a flagella called the axoneme (hence the name axonemal dynein). Each doublet microtubule is made up of an A MT (a complete MT with 13 protofilaments) with a B MT attached to it (an incomplete MT with only 10 protofilaments). These two MTs attached together is the reason why the complex is called a "doublet" microtubule. Each doublet microtubule (dMT) has two rows of dynein molecules attached along its A tubule which then bind to and produce motion on its neighboring dMT's B tubule. Since dMTs in the axoneme are fixed together where the flagella attaches to a cell, dynein induced shearing of adjacent dMTs distal to this point causes the axoneme to bend. The axoneme (see Figure 1.1) is generally made up of nine

dMTs (with outer dense fibers between them and the fibrous sheath around the axoneme) surrounding two single MTs (called the central pair). Each adjacent pair of dMTs is connected by nexin links while all of them are connected to the central pair through radial spokes. The placement of inner and outer arm dynein on the dMTs can also be seen in Figure 1.1. Dynein has been shown to be minus end directed, meaning that it generates force that moves it toward the minus end of a MT. All of the dMTs in an axoneme have their minus ends at the basal end of the flagella by the attachment to the cell. Thus, as dynein "walks" towards the minus end of one dMT, it pushes its adjacent dMT away from the base.

While it is clear how the dynein molecules shearing adjacent dMTs in the axoneme [Brokaw, 1989] cause a bending of the dMTs, the mechanism underlying the generation of propagated waves of flagellar/ciliary motion has yet to be fully understood, especially with regard to the magnitude and regulation of the forces produced by dynein. Our experiments are guided by one of the most powerful and widely cited models for predicting flagellar/ciliary motion: the Geometric Clutch Model [Lindemann, 1994]. This model proposes that a transverse force produced by the flagellar bending causes a separation of the dMTs which disengages sections of dynein, thereby alternating which side of the flagella is active to produce cyclical flagellar bending; first one way, then the other. Central to this model is the hypothesis that axonemal dynein can produce enough force per length of axoneme to generate a transverse force sufficient to detach dynein; this causes dynein motors to be cyclically activated and inactivated [Lindemann, 2003].

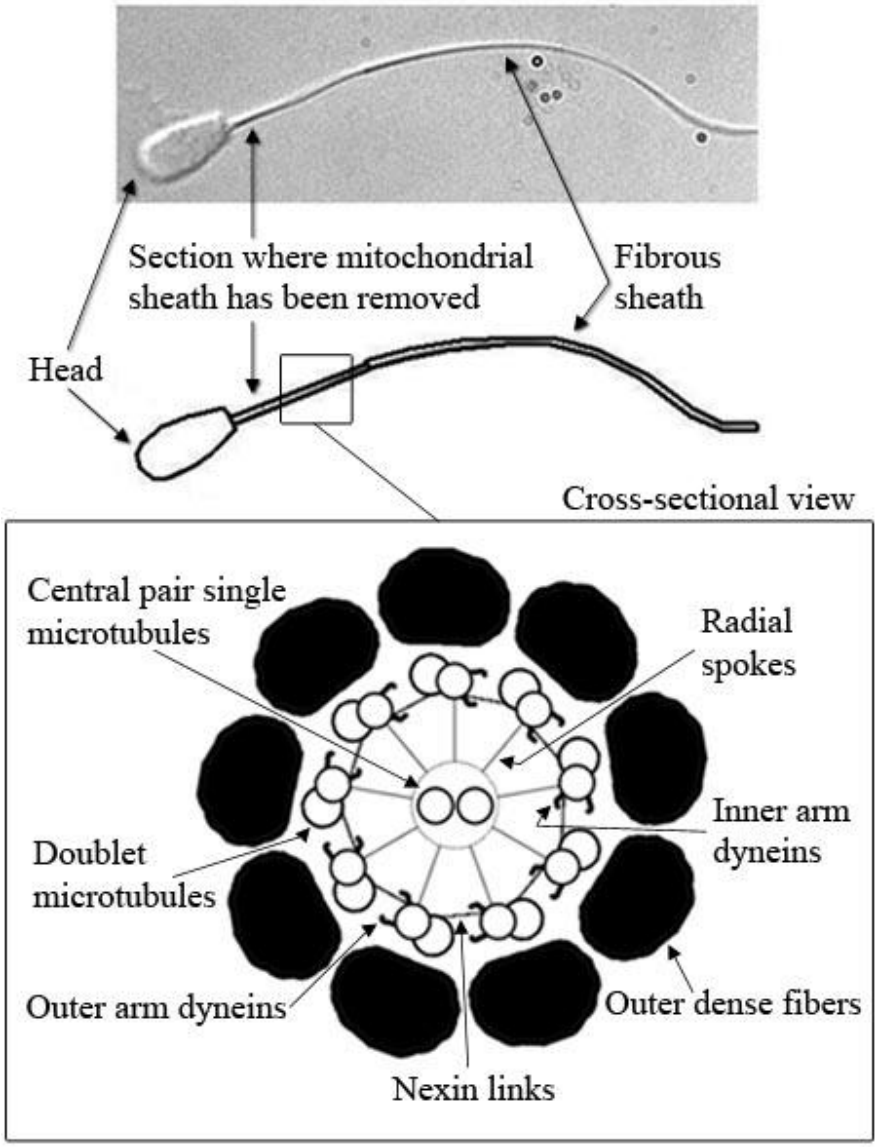

Figure 1.1: A Demembranated Bovine Sperm

A demembranated bovine sperm with its mitochondrial sheath removed along with a cross-sectional area of an axoneme.

1.4 Dynein Structure & Regulation

Axonemal dynein is a large multi-subunit motor protein. Current evidence suggests that each dynein 380 kDa heavy chain contains a fully functional motor domain (the globular "head") that is composed of six AAA modules formed from 2350 residues of the C-terminal end of the chain [Mocz and Gibbons, 2001]. In flagella of metazoans, which include mammalian sperm flagella, each outer dynein arm contains two heavy chains, and the arms repeat at 24 nm intervals along the dMTs. Six unique inner arms are arranged in a pattern that repeats every 96 nm [Goodenough and Heuser, 1985]. Five of these contain a single heavy chain and one inner arm has two (dynein I1 also called dynein f). The dynein motors act as the primary force producers for flagellar and ciliary motion. The biochemistry of the dynein ATP-hydrolysis cycle has been studied in reduced assays [Oiwa and Sakakibara, 2005], and some studies of motility have been performed using dynein isolated from non-mammalian axonemes [Hirakawa et al., 2000; Sakakibara et al., 1999], but relatively little has been done to study mammalian, axonemal dynein in a reduced, chemically controlled environment. This is mostly because isolating functional dynein from mammalian axonemes has proven difficult. The structure of the mammalian axoneme has evolved several differences from non-mammalian axonemes such as the addition of a fibrous sheath, a mitochondrial sheath, and outer dense fibers. As mammalian dynein has been subject to relatively little study in reduced systems, it is unclear if further differences are present at the level of motor functioning.

While there are two major classes of dynein: cytoplasmic and axonemal, even species within these classes have been shown to have varied properties. Within an axoneme, the inner and outer arm dyneins can be morphologically as well as functionally different. Also, even inner and outer arm dyneins can be different dependent on what organism they are within. There are, of course, some common structures amongst the family. Axonemal dynein contains a "stem" which is permanently attached to its respective dMT. On that stem are 1, 2 or 3 heads (dynein heavy chains) each attached to a "stalk" (aka "B-link"), which contains a MT binding site at its end for attaching to that dynein's neighboring dMT. The dynein head is where ATP hydrolysis takes place. Unlike kinesin and myosin, the location of ATP hydrolysis for dynein is quite a distance (approximately 20 nm) from the location of MT binding [Burgess et al., 2003; Lindemann and Hunt, 2003]. In addition to this being a relatively long distance, the B-link that is between these two points of contact is fairly flexible having a maximum stiffness of 0.47 pN/nm with the stem having a maximum stiffness of 0.1 pN/nm [Burgess et al., 2003] resulting in a total series stiffness of only 0.08 pN/nm. This is not viable to support flagellar motility if the stem is the only support mechanism for dynein [Lindemann and Hunt, 2003]. These issues raise many questions about how dynein is able to transfer the force required for movement to its adjacent dMT.

In addition to the complication of dynein's curious force transduction from the site of ATP hydrolysis to the tip of the B-link, this ATP hydrolysis site is not the only nucleotide binding site on the heavy chain. There are actually four nucleotide binding sites on each heavy chain with only one of them being the site of ATP hydrolysis (for

review see [Asai and Koonce, 2001]). These three "extra" sites are believed to have some sort of regulatory nature [Kikushima et al., 2004; Kinoshita et al., 1995b; Shiroguchi and Toyoshima, 2001; Yagi, 2000]. In the presence of ATP, addition of ADP has been shown to increase MT translocation extent of sliding [Kinoshita et al., 1995b], velocity [Yagi, 2000], acceleration [Kikushima et al., 2004], and ATPase activity [Shiroguchi and Toyoshima, 2001]. If ADP were simply competing for the hydrolysis site, these effects would not be expected. Assuming that the additional nucleotide binding sites somehow influence the catalytic activity of the hydrolysis site, these observations obtain greater clarity. In some cases, ATP at higher concentrations has even shown an inhibitory effect on axonemal dMT extrusion [Kinoshita et al., 1995b]. This would imply that dynein acts in a non-Michaelis-Menten kinetics fashion for some aspects of its motion. The inhibitory effect of higher ATP concentrations has been suppressed with the addition of ADP in some *Chlamydomonas* mutants [Omoto et al., 1996]. These evidences strongly support the thought that the multiple nucleotide binding sites on dynein must be regulatory. A better understanding of the activities and biochemistry of nucleotide binding is necessary to see the inner workings of dynein as a tightly regulated nano-scale motor.

1.5 Relationship to Medical Interests

Knowledge about axonemal dynein will benefit clinical applications such as the treatment of disease and control of fertility. One such disease is Primary Ciliary Dyskinesia (PCD) which results in respiratory problems and even infertility due to axonemal defects. Studies have shown that current diagnoses based off of ciliary beat frequency (the number of beats per unit time) can be improved by using ciliary beat

pattern (the overall shape of ciliary movement) [Chilvers et al., 2003]. If flagellar/ciliary motion were better understood, the ciliary beat patterns for PCD could be better distinguished which could lead to improved diagnoses for this disease.

In addition to treatment of disease, the physiology of fertility will be better understood with improved knowledge about axonemal dynein. For instance, chemotaxis of the sperm to the egg within mammals. The exact process for this is not well understood, but is thought to be related to hyperactivation (asymmetric bending and greater amplitude of sperm flagellar waveforms) which has been linked to calcium concentration [Ho et al., 2002]. Before sperm are hyperactivated within the female reproductive tract, they are first activated (become motile) within the male epididymis. Inactive sperm from the epididymis of rats has been activated using calcium and/or cAMP [Armstrong et al., 1994]. These important milestones in the life of a sperm's motility may be due to a direct influence of chemical factors such as calcium and cAMP within the flagella on dynein itself rather than the axoneme as a whole. By studying the optimal assay conditions for MT translocation by dynein, a better insight can be gained into how processes like activation and hyperactivation occur within the realm of mammalian fertility down to the molecular level of dynein.

CHAPTER 2

DYNEIN'S MOVEMENT OF FREE MICROTUBULES

To better understand axonemal dynein's role in the intricately coordinated motion of flagella and cilia, we use an *in situ* assay in which fluorescently labeled single MTs are observed gliding along dMTs from disintegrated bovine sperm flagella. This allows study of exposed, active dynein while they are still attached to their natural substrate: the dMTs, and presumably attached in a physiologic geometry as suggested by electron micrographs and tomography of the dMTs from *Tetrahymena*, *Chlamydomonas*, and sea urchin sperm [Avolio et al., 1986; Nicastro et al., 2006; Sugrue et al., 1991; Sui and Downing, 2006].

2.1 Materials & Methods

2.1.1 Treatment of Bovine Sperm

Preparation and use of bovine sperm for direct study of the mammalian axoneme follows established procedures. Removal of the membrane is performed by exposing the sperm to 0.1% Triton X-100 detergent [Lindemann and Schmitz, 2001], and mitochondrial sheaths are removed using a freeze/thaw cycle [Lindemann et al., 1980]. When the structural integrity of bovine sperm is disrupted by removing their membranes and mitochondrial sheaths, the action of dynein motors in the presence of ATP no longer

causes bending, but instead causes disintegration, and dMTs are extruded out of the proximal 12 microns of the flagellum, where the mitochondrial sheath has been removed. This disintegration exposes dynein, which is still bound to the extruded dMTs.

2.1.2 Preparation of Fluorescent MTs

α–β tubulin dimers are extracted from bovine brain by three cycles of polymerization and depolymerization and purification on a phosphocellulose column, then frozen [Howard et al., 1993; Weingarten et al., 1974]. Cycling is repeated to remove any denatured protein off the column. In some studies, tubulin is purified without a column using high-molarity cycling [Castoldi and Popova, 2003]. Tubulin is fluorescently labeled through addition of tetramethylrhodamine-succinimidyl ester, and again run through cycles of polymerization and depolymerization [Hyman et al., 1991]. GTP and $MgCl_2$ is added to a mixture of labeled and unlabeled tubulin in BRB80 buffer and incubated at 37° C to polymerize the tubulin into MTs; subsequently taxol is added to stabilize the MTs for use.

2.1.3 The Gliding Assay

Bovine sperm, with membranes and mitochondrial sheaths removed, are either left suspended in the demembranation solution and observed under a glass coverslip preparation (where the coverslip is simply dropped on top of the sample on the glass slide), or the solution is exchanged after the axonemes settle onto the cover slip of a chamber constructed of a cover slip and glass slide separated by two strips of double-sided tape. For the coverslip preparation observations, the demembranation solution (20

mM Tris buffer at a pH of 7.8, 132 mM sucrose, 24 mM K-Glutamate, 1 mM $MgSO_4$, 1 mM DTT, 0.1% Triton X-100, 0.5 mM EGTA, 5 mM sodium citrate, and 10 μM cAMP) is converted to motility buffer to observe MT gliding by adding 10 μM taxol, anti-fade solution (600 μg/mL glucose oxidase, 30 mM glucose, and 120 μg/mL catalase) to prevent photodamage and bleaching, 1 mM $MgCl_2$, ATP, and fluorescent MTs. The addition of ATP initiates disintegration of the axonemes and subsequently supports MT gliding along dMTs. For the chamber observations, the axonemes are disintegrated upon exchanging the demembranation solution with a disintegration solution of 50 mM Tris buffer (pH 7.8), 1 mM EGTA, 1 mM $MgCl_2$, and 0.01 or 1 mM ATP. Once disintegration takes place (10 minutes or less), this disintegration solution is exchanged with a motility buffer solution of 50 mM Tris buffer (pH 7.8), 1 mM EGTA, 10 μM taxol, anti-fade solution, 1 mM $MgCl_2$, ATP, 1 mM DTT, and fluorescent MTs. The ATP in the motility buffer solutions is varied as detailed below. After adding motility buffer, samples are viewed under a microscope with DIC and fluorescent imaging capabilities. Images of fluorescent MT movement along dMTs are analyzed using ImageJ (an NIH open-source image processing and analysis software) to measure their gliding velocities. MT gliding velocities are calculated only for periods of constant motion moving away from the basal end of the flagella. For any data analysis involving MT length, the entire length of the MT was in contact with the dMT throughout the motion.

Initially, gliding assays were performed in coverslip preparations in the same solution in which the bovine sperm were demembranated and stored. In this case MT gliding velocity exhibits a time-dependent decrease, slowing to half the initial speed

within 5 minutes. The decrease in gliding velocity can be prevented by adding an ATP regenerating system (2 mM phosphoenolpyruvate and 0.1 mg/mL pyruvate kinase) to the experimental solutions, indicating that slowing is due to depletion of ATP. This depletion is apparently due to MT-dependent ATPase activity, since when the axonemes and ATP are pre-incubated for 30 minutes after disintegration before MTs are added, the velocities are similar to gliding velocities immediately after disintegration. This unexpectedly large MT-dependent ATPase activity is much higher than is expected from dynein activity alone; the total number of axonemal dyneins in an assay slide are of the order of a few billion, and even if all were actively hydrolyzing ATP at 100 s^{-1}, the depletion of the 1 mM ATP in the 7 µl sample volume would be negligible. Thus to avoid ATP depletion by unidentified, presumably soluble MT-dependent ATPases, we switched to using flow chambers to allow fluid exchange to remove any soluble enzymes leftover from when the axonemes were demembranated. With this procedure, the MT gliding velocity does not decrease over time, indicating that rapid ATP depletion is indeed due to soluble enzymes, and allowing well-controlled study of the relation between gliding velocity and the ATP concentration.

2.2 Results

2.2.1 Diverse MT Movement

We find that fluorescent MTs added to extruded dMTs immobilized on coverslips exhibit ATP-dependent gliding as they are propelled along rows of dynein motors on the dMTs. Movements were characterized by tracking the gliding MTs through a series of

successive images (Figure 2.1). The character of MT interactions with the dMTs is variable (Table 2.1), but most commonly MTs associate laterally with dMTs all along the MTs' length, and remain immobilized at the attachment location. Some MTs become attached at a point crossing the dMT and rotate back and forth around that point; often these MTs dissociate from the dMT after a period of attachment, and in some cases are translocated over the point of attachment. This rotation suggests these MTs may be attached to a single motor, and swivel about the motor as they are propelled. The MTs that glide along a dMT exhibit variable characteristics of motion. Often a gliding MT displays periods of motion interrupted with stops, producing a stuttering movement, or the MT stalls at the leading end, causing it to buckle as the trailing end continues to move. MTs would often glide past another immobilized MT on the dMT. This likely reflects the gliding MT being propelled along one set of either the inner or outer arm rows of dynein on the dMT, while the stationary MT was on the other row.

Notably, MT gliding sometimes proceeds in the non-physiologic direction toward the base of the axoneme (where the minus ends of the dMTs are located) (Figure 2.1b), and occasionally the direction of MT gliding oscillates over short distances, switching between movement toward and away from the base of the axoneme. These behaviors are surprising, as in the normal state of a functional axoneme, dynein on one dMT pushes its adjacent dMT away from the basal end of the axoneme due to minus end directed activity of dynein motors. These variabilities may reflect properties of flagellar dynein that allow oscillatory bending of flagella, which require dMTs to cycle between sliding past each other in opposite directions.

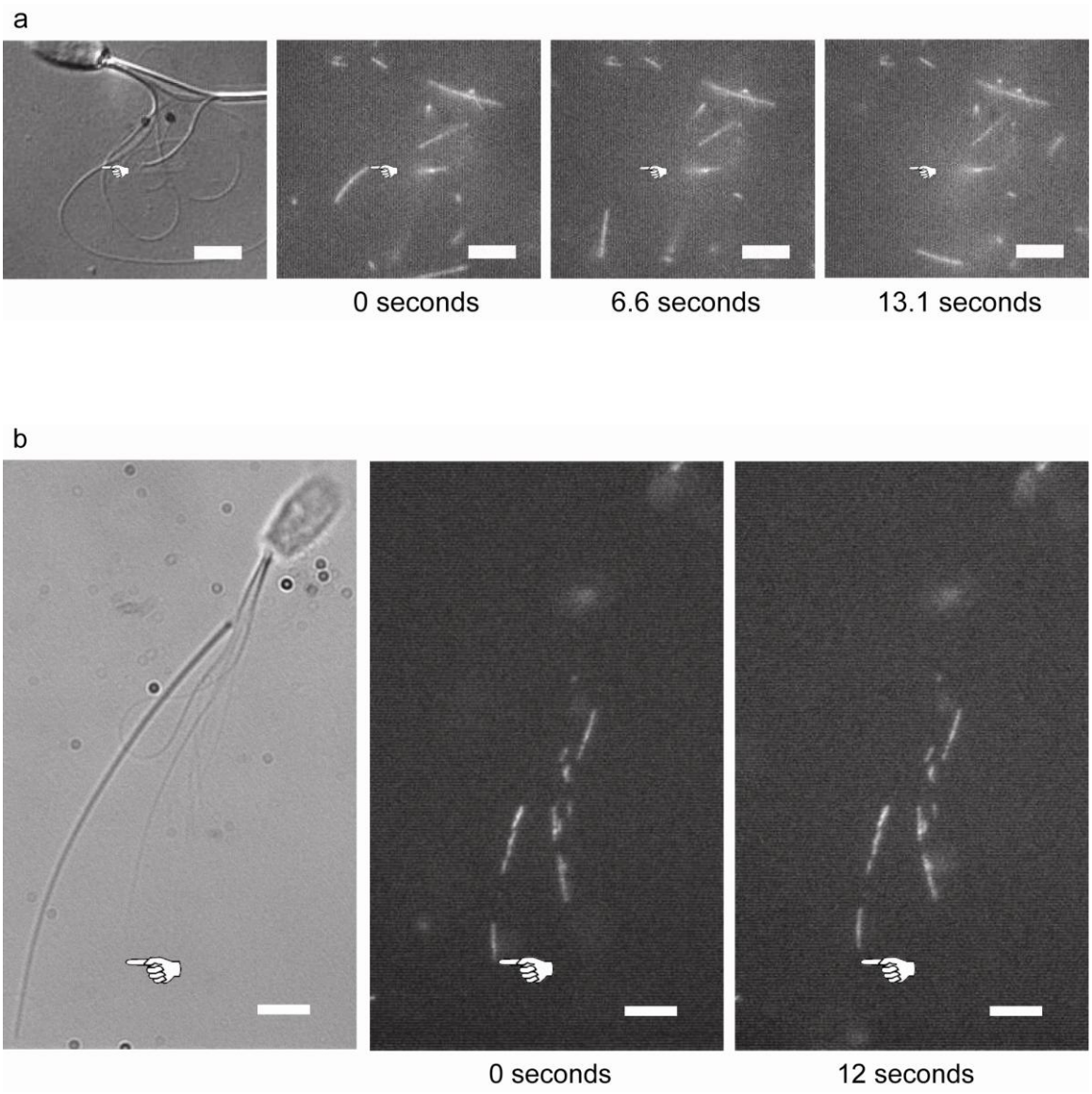

Figure 2.1: Movement of Fluorescent MTs Along Mammalian dMTs

These assays were performed at ATP concentrations of 0.05 mM (a) and 1 mM (b). The left panel in each sequence is a DIC image of the disintegrated axoneme. The following images are samples of fluorescent images (taken every 200 or 300 msec) showing MT movement over time. The hand in each image points to the starting location of the moving MT. The MT in (a) is moving away from the base of the axoneme and did not move continuously, exhibiting starts and stops throughout its translocation. Prior to this MT's first stop, its velocity was ~1.2 μm/sec. The MT in (b) is moving ~1.4 μm towards the base of the axoneme at a velocity of ~0.1 μm/sec. Bar = 5 μm.

MT Gliding Characteristic	% of Gliding MTs (N = 879)
Translocation towards the flagellar base	< 1% (7)
Oscillating	~2% (16)
Buckling	< 1% (8)
Stuttered motility	~9% (81)

Table 2.1: Frequency of MT Gliding Characteristics

2.2.2 ATP Dependence

ATP-dependent MT gliding follows Michaelis-Menten kinetics, with a maximum velocity of 4.7 ± 0.2 μm/sec and a K_m of 124 ± 11 μM (Figure 2.2). This is fairly consistent with axonemal dynein behavior observed in many mammalian [Bird et al., 1996] and non-mammalian [Kurimoto and Kamiya, 1991; Shiroguchi and Toyoshima, 2001; Yamada et al., 1998] systems as summarized in Table 2.2. Since it has previously been proposed that ADP may regulate dynein's activity at a second allosteric binding site [Kinoshita et al., 1995a; Shiroguchi and Toyoshima, 2001], we examined the velocity of MT gliding in the presence of ADP, finding decreased gliding velocity with the addition of 100 μM to 500 μM ADP; velocities, respectively 1191 ± 24 nm/sec and 1061 ± 56 nm/sec, are compared with the 1364 ± 70 nm/sec at the same ATP concentration (0.05 mM) without added ADP.

2.2.3 Lack of Dependence on Motor Number

An advantage to examining motor activity on dMTs is that the motors are distributed with uniform spacing [Nicastro et al., 2006; Sui and Downing, 2006], and thus the number of motors acting on a MT is expected to scale in direct proportion to the MT length. Thus, cooperative or interfering activities between multiple motors acting on a single MT may be indicated by length-dependent changes in the motility behavior. Examining the correlation of MT length and gliding velocity (Figure 2.3), we find that the slopes are not significantly different from zero, implying that there is no relationship between MT length and gliding velocity. Thus for these ensembles of dynein arms under low load, the gliding velocity is independent of the number of interacting arms, at least

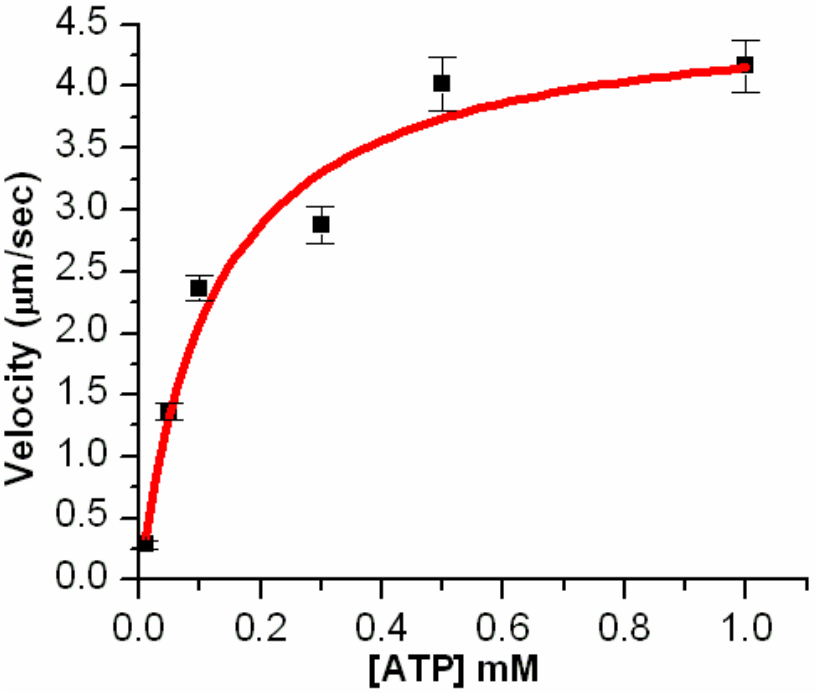

Figure 2.2: MT Gliding Velocity ± SE Versus [ATP]

Curve is fit to Michaelis-Menten, V_{max} = 4.7 ± 0.2 µm/sec and K_m = 124 ± 11 µM. Each data point was calculated from 7 to 19 MT translocations.

Dynein Species	Assay Type	[ATP]	Km	Velocity	Reference
Bovine (Inner & Outer Arms Present)	MTs Gliding on Dynein on Doublet MTs	0.01 to 1 mM	124 ± 11 μM	Vmax = 4.7 ± 0.2 μm/sec	Current Work
Bovine (Inner & Outer Arms Present)	Disintegration	0.02 to 2 mM	N/A	~2 to ~8 μm/sec	Bird et al., 1996
Tetrahymena (Only Inner Arm A Present)	MTs Gliding on Dynein Removed From Doublet MTs	0 to 2 mM (+ 20 μM [ADP])	350 ± 10 μM	Vmax = 6.6 ± 0.1 μm/sec	Shiroguchi and Toyoshima, 2001
Sea Urchin (Inner & Outer Arms Present)	MTs Gliding on Dynein on Doublet MTs	0.1 mM	N/A	3.1 ± 2.1 μm/sec	Yamada et al., 1998
Chlamydomonas (Inner & Outer Arms Present)	Disintegration	0 to 0.5 mM	177 μM	Vmax = 25.6 μm/sec	Kurimoto and Kamiya, 1991

Table 2.2: Summary of Axonemal Dynein Assays

Summary of axonemal dynein disintegration and gliding assays for different species.

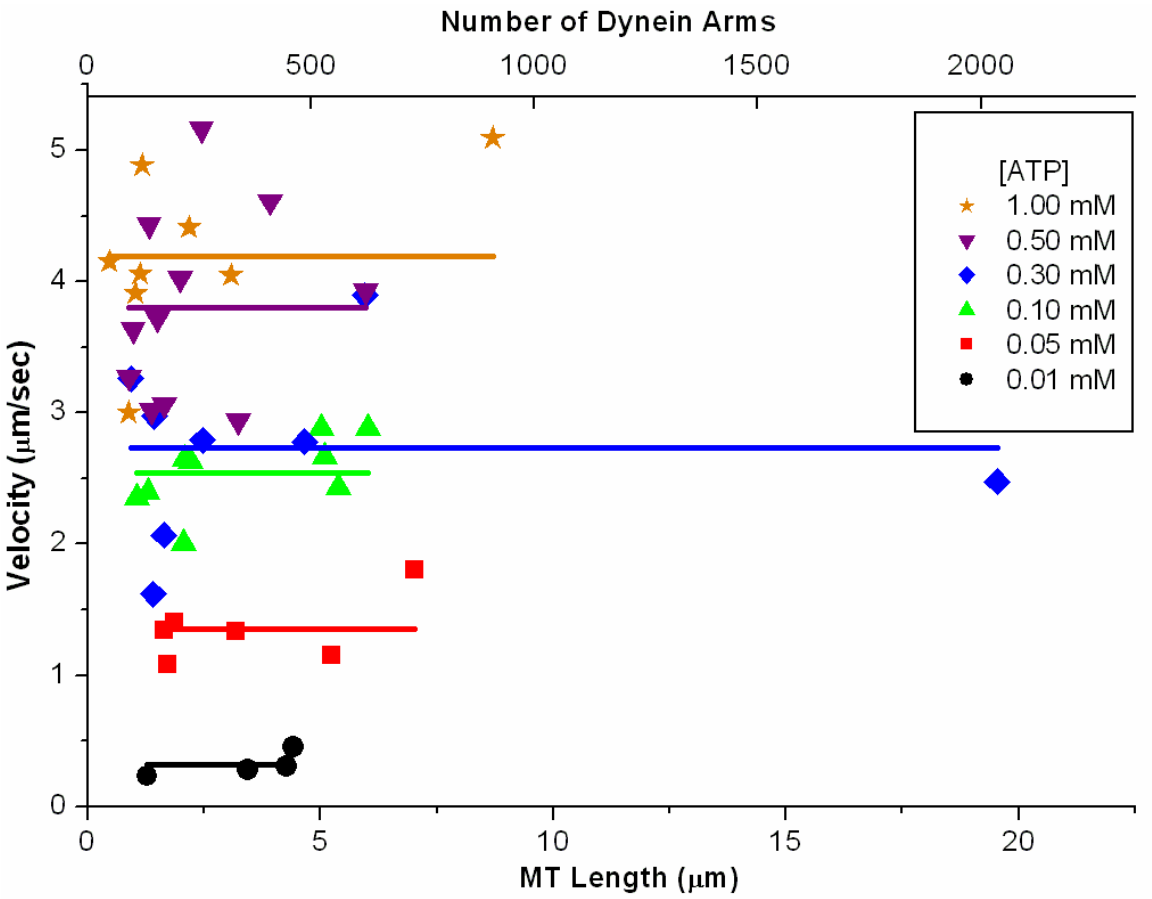

Figure 2.3: MT Gliding Velocity is Independent of Length

The number of motors potentially propelling a MT was estimated by assuming 41.7 outer dynein arms (83 dynein heads) plus 62.5 inner dynein arms (73 dynein heads) along 1 μm of dMT. Thus, the number of motors acting on a MT gliding along the dMT is expected to vary in proportion to the MT length. Lines are average velocity; the slopes of regression fits for each ATP concentration were not significantly different from zero. Each data point was calculated from 4 to 11 MT translocations.

when the number of arms is in excess of about 49, the number of dynein arms expected to act on the shortest observed MTs (~0.5 μm).

2.3 Discussion

The chemomechanical details of dynein motor activity are central to establishing the oscillatory bending of the flagellar axoneme. Currently there is no way to remove vertebrate dynein from the rest of the axoneme while retaining functionality for experimentation in reduced assay systems, as has been done for cytoplasmic dynein [Mallik et al., 2004] or non-mammalian, axonemal dynein [Kikushima et al., 2004]. To address this, we have established an assay in which MTs are propelled by mammalian flagellar dynein motors, which retain their attachment to extruded dMTs. In this assay, fluorescent MTs glide along axonemal dynein [Yamada et al., 1998], allowing direct observation of the activities of these nanoscopic motors. Table 2.2 summarizes several studies of dynein using a variety of assays and organisms (our current work is highlighted). The maximum velocity in our gliding assays (4.7 ± 0.2 μm/sec) is consistent with observations of bovine sperm axoneme disintegration, where the velocity of extruding dMTs was measured in the range of about 2 to 8 μm/sec [Bird et al., 1996]. Note that for consistency in comparisons, in the present study MTs that were observed oscillating or gliding toward the head were excluded from calculations of average velocities. We find the velocity and K_m values are close to other dynein species despite the multi-Kingdom diversity of these organisms [Kurimoto and Kamiya, 1991; Shiroguchi and Toyoshima, 2001; Yamada et al., 1998].

Our finding that the addition of ADP decreases MT gliding velocity contrasts with previous studies in which ADP increased the extent of MT sliding [Kinoshita et al., 1995a], the gliding velocity [Yagi, 2000], the gliding acceleration [Kikushima et al., 2004], and the ATPase activity [Shiroguchi and Toyoshima, 2001]. What might account for this difference? It has been hypothesized that ADP's influence is through a second nucleotide binding site on each dynein head, having a higher affinity for ADP than ATP [Shiroguchi and Toyoshima, 2001]; if this site allosterically regulates ATPase activity at the primary ATP binding site, a complex relationship could exist between dynein activity and ATP/ADP concentration. Such a relation has been hypothesized to explain the previously observed increase in ATPase activity and motility in the presence of ADP, contrary to the expected decrease in the simplest enzymatic models. As we find no evidence for increased dynein activity in the presence of ADP, it may be that mammalian dynein is simply different from protists in this respect, or it may be that ADP's influence is dominant in certain classes of dynein within an axoneme. Possibly, the effect of ADP on a subset of mammalian dyneins are overwhelmed by the unaffected motors at the density and proportions in our assays.

Unexpectedly, MTs sometimes glide in the non-physiologic direction toward the base of the axoneme, and occasionally oscillate over very short distances. Such non-physiologic gliding presumably occurs when a MT associates with a dMT such that the plus end is near the base of the axoneme, opposite the physiologic orientation. However, additional factors must be involved since this reverse motion occurred rarely, rather than ~50% expected if gliding direction was solely determined by MT landing orientation.

Possibly only a subset of dynein motors can support plus-end directed motion so that "backward" motion ensues only when a MT both lands reversed from physiologic orientation and fortuitously associates with a large proportion of this subset of motors, perhaps all located on one of the dynein rows (inner or outer). This is consistent with the significant quantity of MTs that associate with a dMT but remain immobile, which then may reflect backward MTs that associate with a sufficient proportion of motors that cannot support motility in a non-physiologic direction. As the inner arms are predominantly single headed, perhaps only the inner arms are sufficiently flexible for attachment when the MT is oriented in the reverse direction. In any case, the observation of backwards movements indicates that at least a subset of motors contains sufficient compliance to associate with and propel a MT that is oriented 180 degrees from the normal direction. Though this has not been previously described for dynein, and may at first seem surprising, similar behavior has been observed for both myosin [Sellers and Kachar, 1990] and kinesin [Hunt and Howard, 1993] motors. The number of dynein motors near a MT that are capable of swiveling 180 degrees may influence whether the MT is able to glide a short distance in the wrong direction or even oscillate back and forth. Oscillatory behavior has also been observed for a non-mammalian axonemal dynein under loads applied using optical tweezers [Shingyoji et al., 1998]; though in that study, the MT was interacting with 1-4 dynein arms whereas in our study even the shortest oscillating MT is likely associated with ~10 times that many. We note that the oscillatory motions we observe, which typically occurred over short distances (< 1 μm in either direction), could potentially be due to activities involving non-motor structures, such as elastic relaxation, or the MT interacting with a loose, wobbling dMT. Thus, these

oscillations do not necessarily indicate that dynein can switch directions relative to the polarity of the translocated MT even though the MTs can oscillate along the tracks of dynein.

Since the number and arrangement of motors present on the dMT is known [Nicastro et al., 2006; Sui and Downing, 2006], we can predict the number of motors that can potentially act against the length of the gliding MT. The dependence of gliding speed on motor numbers has also been examined in studies of kinesin, myosin, and non-mammalian dynein. Conventional kinesin has been found to be independent of the number of motors present [Howard et al., 1989] while the speed that myosin propels actin has been found to increase with increasing numbers of motors at low motor densities [Uyeda et al., 1991]. Likewise, the speed that non-mammalian dynein translocates MTs increases with the number of motors [Hamasaki et al., 1995]. Similar to the kinesin studies, our results indicate that for mammalian flagellar dynein the MT velocity is independent of the number of motors, at least above ~49 dynein arms. While the speed of MTs propelled by non-mammalian dynein has been shown to depend on the number of motors, this is only apparent when the estimated number of motors ranged near or less than our lowest observations. Since the drag on a sliding MT is very low, on the order of femtonewtons [Hunt et al., 1994], the independence of speed and motor number reflects an intrinsic upper limit on dynein velocity, presumably due to synchronization of hydrolysis cycles of dynein motors acting on the same MT.

Control of motion at the nanoscale is a central obstacle for developing practical nano- and micromechanical devices. A number of studies have examined the use of patterned tracks of motor proteins to guide movements [Clemmens et al., 2003; Hess et al., 2001; Hoff et al., 2004; Reuther et al., 2006; Riveline et al., 1998], but it has been a challenge keeping movements following patterned motors, especially if they are not in a straight line; the use of barriers produced through lithography is necessary to guide filament cargoes along bends [Hiratsuka et al., 2001; Moorjani et al., 2003]. The need for barriers may reflect the requirement of geometry and high density for a filament to be moved along a tight curved line. Dynein motors arrayed along dMTs are able to guide MTs along a curved track, demonstrating that with sufficient density and organization, motors can guide MTs along bends without being guided by mechanical barriers. Potentially, extruded dMTs could be used as cargo tracks for actuating nano- and micromechanical devices.

We have examined the movement of MTs along extruded dMTs from bovine sperm flagella. Gliding MTs displayed a range of motile behaviors, including backwards movements, that provide insight into diverse behaviors of mammalian axonemal dynein motors, and how they operate together while still attached to their natural substrate. We found that MT gliding velocity was independent of the number of dynein motors present along the dMT, and did not display evidence for increased activity due to ADP regulation. This reduced assay allows dynein motility to be studied in a controlled environment, while retaining their attachment to dMTs. This assay also allows the forces generated by mammalian dynein to be studied in ongoing biophysical assays.

CHAPTER 3

DYNEIN'S MOVEMENT OF LOADED MICROTUBULES

There have been several successful attempts at directly measuring dynein's force and translocation using optical tweezers, but none of these have used mammalian axonemal dynein or any vertebrates *in situ*. Cytoplasmic dynein and non-mammalian axonemal dynein have been used in optical tweezers assays by placing the protein on a slide, *in situ* on the doublet MT, or directly adsorbed to a bead held in an optical trap. In these studies, it was possible to measure lateral movement along MT protofilaments [Wang et al., 1995], processivity [Hirakawa et al., 2000; Sakakibara et al., 1999], step size [Hirakawa et al., 2000], and force [Mallik et al., 2004; Shingyoji et al., 1998]. In one of these studies, single outer arm dyneins of Tetrahymena were shown to be processive only at low ATP concentrations (about 3 μM) while non-processive at higher ATP concentrations (about 20 μM) [Hirakawa et al., 2000]. In another study cytoplasmic dyneins were shown to have an increasing stall force with increasing ATP concentrations [Mallik et al., 2004]. Although none of these studies used mammalian axonemal dynein, they are excellent models for experimenting with dynein using optical tweezers. However, it is expected that there will be substantial differences in the behavior of flagellar dynein, which works in organized arrays, versus cytoplasmic dynein which works individually or in small numbers. Furthermore, the force of small numbers of dynein motors or motors operating *in situ* on doublet microtubules has only been the

subject of one study in protists [Shingyoji et al., 1998] and has never been examined in vertebrates. In our optical tweezers study, we have gained a further understanding of some of these properties (such as processivity, step size, and force) for small numbers of mammalian axonemal dynein for various [ATP] and [ADP] conditions.

3.1 Materials & Methods

3.1.1 Doublet and Single MT Preparations

Doublet MTs from bovine sperm were extruded as described [Lorch et al., 2008]. α–β tubulin dimers were prepared as described [Lorch et al., 2008] except without being fluorescently labeled. Single MTs from α–β tubulin dimers were prepared as described [Lorch et al., 2008] except with biotin-succinimidyl-ester added to biotinylate the MTs for attachment to neutravidin-coated beads. The biotin (for a final concentration of 2 mM) was added to the polymerized MTs and then were incubated for 15 mins at 37° C. Glycine at a final concentration of 300 mM was then added to quench the still lose biotin and the MTs were sent through 3 rounds of centrifugation to remove any lose glycine-bound biotin. When necessary, single MTs were sheared through a 10 uL pipetteman and/or a 25 gauge needle immediately before use.

3.1.2 Coating Beads With Neutravidin

Silica beads (diameter = 0.57 μm) were suspended in BRB-80 at 10 mg/mL. This solution then had biotin-BSA added to it for a final concentration of 2 mg/mL. The beads were then sent through one cycle of vortexing, pelleting, and washing in BRB-80 for a

final bead concentration of 1 mg/mL. Neutravidin was then added for a final concentration of 20 ug/mL. The beads were then sent through 3 cycles of vortexing, pelleting, and washing for a final bead concentration of 10 mg/mL. Aliquots were flash frozen and stored at -80° C until thawed quickly in a 37° C water bath and sheared through a 25 gauge needle immediately before use.

3.1.3 The Optical Tweezers Assay

Bovine sperm were prepared as described [Lorch et al., 2008]. Demembranated axonemes were put into a cover slip-tape chamber on a slide and disintegration solution exchanged through as described [Lorch et al., 2008] except that prior to slide use, casein at 2 mg/mL was dried onto and then rinsed from the slide surface. This produced a cover slip surface with less risk of beads sticking to the cover slip while they were being positioned near dMTs. For experiments where beads were coated (from now on referred to as the coated-bead assays) (Fig. 3.1a) with MTs, a solution of 2 mg/mL casein was then exchanged through, followed by a solution of 50 mM Tris buffer (pH 7.8) and 10 μM taxol, followed by a motility buffer solution of 50 mM Tris buffer (pH 7.8), 1 mM EGTA, 10 μM taxol, anti-fade solution (600 μg/mL glucose oxidase, 30 mM glucose, and 120 μg/mL catalase), 1 mM $MgCl_2$, ATP, ADP (if being used at the time), 1 mM DTT, 0.3 mg/mL neutravidin-coated silica beads, and biotinylated MTs. Experiments for individual MTs (from now on referred to as the individual-MT assays) (Fig. 3.1b) attached to beads had the same conditions with the exception of a BRB80 buffer being used instead of the Tris buffer above for extended stability of long MTs. The slide is then taken as quickly as possible (within a minute) after addition of the motility buffer to the

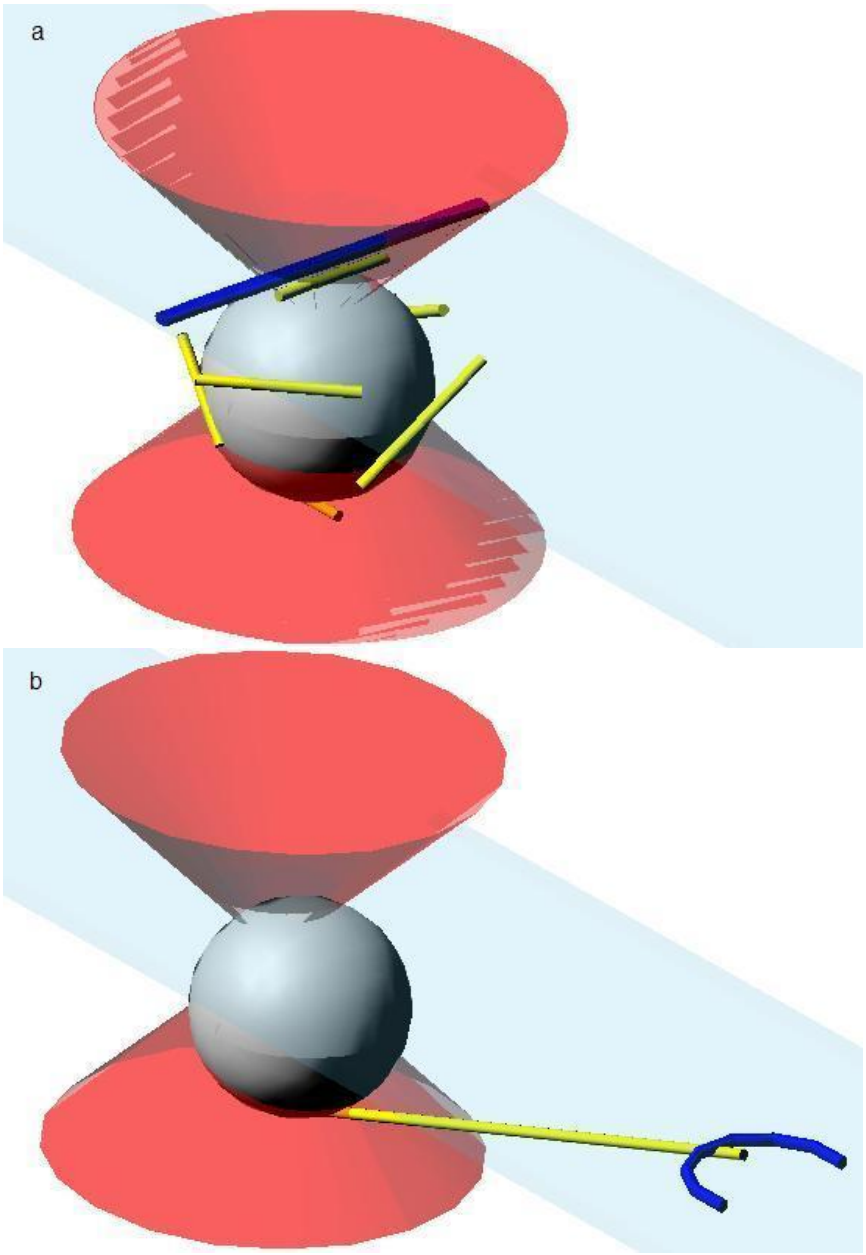

Figure 3.1: Optical Tweezers Assay MT Geometries

Two different geometries of the single MT and doublet MT were used in separate optical tweezers experiments. (a) In the coated-bead assay, the neutravidin-beads are coated with short, single MTs. When the beads are brought into contact with the dMT, the orientation between the single MT and the doublet MT could be parallel (as shown with one of the MTs on the bead) or at any unknown angle. (b) In the individual-MT assay, the neutravidin-beads are found that have an individual, long, single MT attached to it. When the beads are brought close to the dMT, the individual MT is draped across the dMT and the angular orientation can be seen. Gray = silica bead, blue = doublet MT, yellow = single MT, red = optical trap, light blue = cover slip. Diagrams are drawn roughly to scale.

optical tweezers microscope where beads with MTs attached are brought up into contact with exposed dMTs on the cover slip. When the bead is in place, QPD voltage data corresponding to bead position is acquired by LabVIEW software at 5000 Hz [Brouhard et al., 2003].

The optical tweezers are calibrated by using a solution of the neutravidin beads in MQ-H_2O at 0.4 mg/mL, putting that solution into one of the slide chambers, taking the slide to the optical tweezers, catching a bead and bringing it as near to the cover slip surface as it is for the actual experiments, and taking multiple sets of 45 second data traces at the laser powers that were used for experimentation. Sensitivity (voltage relative to distance within the slide chamber) and stiffness (force relative to distance out of the optical tweezers trap) of the trap in the x & y directions are then extracted from these data traces using a power spectral analysis of the variance of the bead's position in the trap due to Brownian motion [Brouhard et al., 2003].

3.1.4 Data Processing & Analysis

Raw data traces (in terms of QPD voltage versus time) are processed through custom written LabVIEW software. First, the data is low pass filtered (at 35 Hz) and then converted to position and force versus time using the optical tweezers calibration data (sensitivity and stiffness) for the laser power that data trace was taken at. The filtered/translated data is then scanned to find dynein displacement occurrences by isolating data where the position went 4 standard deviations (of noise about the zero displacement) away from the center of the trap (zero). The software keeps track of the

direction & magnitude of these displacements and then outputs how many occurred for each trace and the force, velocity, and duration for each dynein-MT displacement.

3.2 Results

Using the two separate geometries (individual-MT versus coated-bead) for the optical tweezers assay (see Materials & Methods), we acquired displacement, force, and duration (the amount of time that each excursion was sustained) measurements from the traces of dynein's movement of the MT-bead combination out of the optical trap. While the coated-bead assay allowed for greater amounts of data to be taken due to being an easier experiment to perform, it did not allow for orientation of the MT to the dMT to be established and therefore left more uncertainty in the number of motors interacting with the MT. The coated-bead assay still have relatively few motor numbers interacting since the MTs were relatively short (less than the bead diameter of 0.57 μm), but the individual-MT assay with the single MT draped across the dMT would have only allowed for 1 to 4 motors to be interacting with it since the MT is only about 25 nm in diameter limiting how many it could interact with (since each outer dynein arm is 24 nm apart while a pattern of six inner dynein arms repeat every 96 nm [Goodenough and Heuser, 1985]).

3.2.1 Duration & Processivity

The motions of dynein interacting with MTs attached to beads rather than their normal neighboring dMTs were measured with optical tweezers. Excursions of the bead-MT combination out of the center of the optical trap were recorded in traces of voltage

(converted to position and force) versus time (Fig. 3.2). Occasionally in both the coated-bead and individual-MT assays, dynein would track for larger displacements and durations (> 100 nm and > 0.5 sec), but for the majority of the excursions, displacements were short in length and time (Tables 3.1 & 3.2). For these excursions (not counting 2 times when the bead was pulled out of the trap by dynein) total distances traveled reached as high as 165 nm, but were more typically 10s of nanometers while durations reached as high as 60 sec, but were more typically 100s of milliseconds. Times that it took to reach maximum distances also for both individual-MT and coated-bead assays were typically on the order of 10s of milliseconds or less (Tables 3.1 & 3.2); too short to calculate average velocities confidently at the rates that the data must be filtered (low pass filtered at 35 Hz). For times (to reach maximum distance) longer than 0.1 seconds, displacements had velocities as low as 3 nm/sec. These longer displacements were observed less often during the individual-MT experiments compared to the coated-bead experiments.

3.2.2 Step Size

While dynein is known to be minus end directed, 44% of optical tweezers traces (49% of coated-bead and 14% of individual-MT) had dynein producing displacements towards both the plus and minus end of the MT as has been seen in our previous gliding assay studies as well [Lorch et al., 2008]. Using only the traces from the individual-MT assays, a statistical analysis was done assuming a binomial distribution for the frequency of dynein displacements outside of the signal noise in either direction of the MT. With dynein being inactive (bound but not producing a displacement), the probability of a displacement outside of the noise in either direction would be equal. In our experiments,

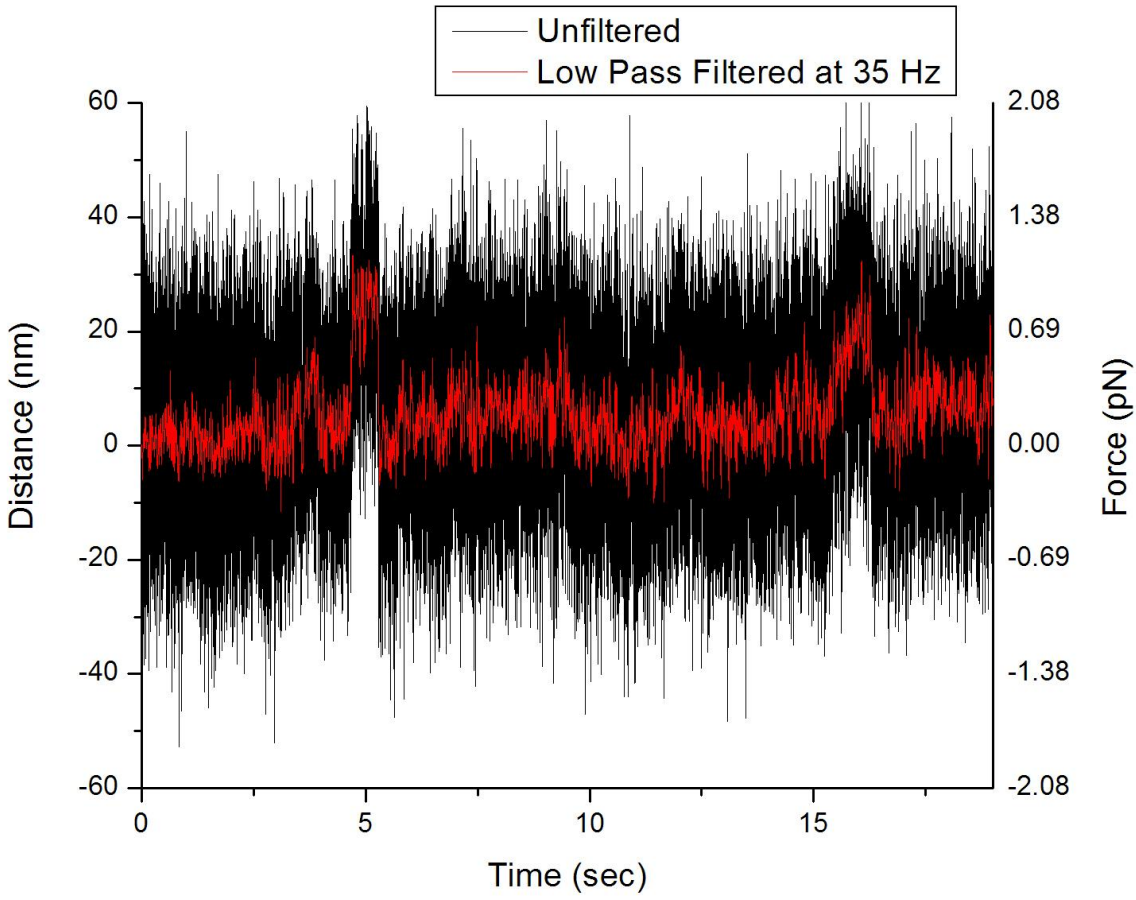

Figure 3.2: Sample Excursions of the MT From the Optical Tweezers Trap

Two excursions of the MT-bead combination from the optical tweezers trap can be seen in this portion of a data trace. This was a coated-bead assay with [ATP] = 0.01 mM and no ADP added. Forces recorded are 1.16 pN (leftmost excursion) and 1.13 pN (rightmost excursion). Black is the unfiltered data trace while red is the data trace after being low pass filtered at 35 Hz.

	Coated Bead (Without ADP)															
	Number of traces:	28														
	Number of excursions:	184			Percent of excursions < 100 nm:	99			Percent of excursions < 0.01 sec:	35			Percent of excursions < 0.5 sec:	88		
[ATP] (mM)	Force (pN)		STD	STE	Max	Displacement (nm)	STD	STE	Max	Time to Max (sec)	STD	STE	Max	Time Sustained (sec)	STD	STE	Max
0.01		0.68	0.31	0.06	1.35	50.56	40.80	8.51	165.04	0.928	2.639	0.550	10.619	0.360	0.435	0.095	1.695
0.05		0.69	0.24	0.05	1.50	56.08	13.00	2.71	83.51	0.023	0.022	0.005	0.086	0.127	0.176	0.037	0.753
0.10		0.59	0.17	0.02	1.28	38.60	13.39	1.46	68.68	0.375	2.092	0.228	14.106	1.514	7.171	0.782	59.574
0.50		0.61	0.15	0.03	0.88	28.38	7.44	1.55	42.63	0.028	0.026	0.006	0.091	0.130	0.135	0.028	0.602
1.00		0.55	0.19	0.03	1.15	28.32	15.19	2.73	69.45	0.020	0.033	0.006	0.187	0.215	0.238	0.043	1.040

	Coated Bead (With ADP & 0.05 mM ATP)															
	Number of traces:	10														
	Number of excursions:	82			Percent of excursions < 100 nm:	100			Percent of excursions < 0.01 sec:	40			Percent of excursions < 0.5 sec:	88		
[ADP] (mM)	Force (pN)		STD	STE	Max	Displacement (nm)	STD	STE	Max	Time to Max (sec)	STD	STE	Max	Time Sustained (sec)	STD	STE	Max
0.00		0.69	0.24	0.05	1.50	56.08	13.00	2.71	83.51	0.023	0.022	0.005	0.086	0.127	0.176	0.037	0.753
0.10		0.70	0.14	0.03	1.03	24.63	4.83	0.97	35.94	0.077	0.156	0.031	0.720	0.222	0.265	0.053	1.071
0.50		0.52	0.15	0.04	0.94	14.92	4.15	1.01	26.93	0.337	1.296	0.314	5.367	0.531	1.572	0.381	6.588
1.00		0.55	0.10	0.02	0.83	24.52	9.37	1.48	62.22	0.017	0.013	0.002	0.062	0.285	0.515	0.081	2.356

Table 3.1: Summary of Data for Optical Tweezers Coated Bead Assay

Summary of data for the optical tweezers coated-bead assay for different [ATP] and [ADP].

	Individual MT (With & Without ADP, With 0.05 mM ATP & 0.50 mM ATP)															
	Number of traces:	7														
	Number of excursions:	50			Percent of excursions < 100 nm:	100			Percent of excursions < 0.01 sec:	36			Percent of excursions < 0.5 sec:	86		
	Force (pN)		STD	STE	Max	Displacement (nm)	STD	STE	Max	Time to Max (sec)	STD	STE	Max	Time Sustained (sec)	STD	STE	Max
		0.86	0.15	0.02	1.16	31.57	6.83	0.97	50.31	0.021	0.021	0.003	0.100	0.262	0.283	0.040	1.435

	Individual MT (With ADP & 0.05 mM ATP)															
	Number of traces:	2														
	Number of excursions:	40			Percent of excursions < 100 nm:	100			Percent of excursions < 0.01 sec:	33			Percent of excursions < 0.5 sec:	88		
[ADP] (mM)	Force (pN)		STD	STE	Max	Displacement (nm)	STD	STE	Max	Time to Max (sec)	STD	STE	Max	Time Sustained (sec)	STD	STE	Max
0.00		0.58	0.05	0.02	0.63	40.10	10.93	4.13	50.31	0.012	0.007	0.003	0.023	0.269	0.280	0.106	0.867
0.01		0.90	0.10	0.02	1.13	28.16	3.12	0.57	35.47	0.020	0.019	0.003	0.074	0.288	0.241	0.044	0.851
1.00		0.94	0.13	0.04	1.16	34.17	4.75	1.50	41.93	0.022	0.020	0.006	0.066	0.099	0.071	0.023	0.239

	Individual MT (Without ADP)															
	Number of traces:	5														
	Number of excursions:	10			Percent of excursions < 100 nm:	100			Percent of excursions < 0.01 sec:	50			Percent of excursions < 0.5 sec:	80		
[ATP] (mM)	Force (pN)		STD	STE	Max	Displacement (nm)	STD	STE	Max	Time to Max (sec)	STD	STE	Max	Time Sustained (sec)	STD	STE	Max
0.05		0.58	0.05	0.02	0.63	40.10	10.93	4.13	50.31	0.012	0.007	0.003	0.023	0.269	0.280	0.106	0.867
0.50		0.84	0.13	0.08	0.99	37.12	5.86	3.38	43.87	0.029	0.036	0.015	0.100	0.475	0.560	0.229	1.435

Table 3.2: Summary of Data for Optical Tweezers Individual MT Assay

Summary of data for the optical tweezers individual MT assay for different [ATP] and [ADP].

we can then use the ratio of displacements in the dominant direction to the less frequent direction for when dynein is active to then see how far the distribution of displacement frequency shifts away from zero based on the probability of this ratio occurring. This shift is then the lower limit (due to the series compliance between the dynein, the MT, and the bead) of the step size that dynein has taken to produce this change in ratio of dominant to less frequent displacements. This corresponds to a dynein step size no less than 4.4 nm with no load being applied to it.

3.2.3 Force & Displacement

The optical tweezers assay, whether coated-bead or individual-MT, had several difficulties which made acquiring dynein movements fairly infrequent. To avoid getting the bead stuck to the cover slip, beads could not be brought too close to the slide surface. The farther away the bead was from the cover slip, the less likely a MT on the bead would come into contact and be translocated by dynein on the dMTs (see Fig. 3.1) that were settled on the cover slip. A region between these two extremes was then used where the bead was unlikely to hit the cover slip, but dynein translocations became rarer. This caused longer traces of data to need to be taken to increase the chance that a MT was caught and translated by dynein though it couldn't necessarily be known until afterwards whether excursions actually occurred. In addition, there was also the issue of bead concentration and settling. There was a trade off for concentration of beads: a lower concentration of beads meant that it was less likely that a bead would accidentally get pulled into the optical trap while data was being taken for another bead, but this also meant it was harder to find a bead in the first place before the beads settled to the bottom

surface of the slide chamber where they remained irremovable. At the concentration that made this possible, it created the additional issue of having to either first find a dMT on the cover slip surface and go find a bead and try to bring it back or grab a bead and then have to travel and find a dMT without losing the bead in this travel or catching another bead in the trap. Even with the difficulties listed above, 316 excursions were recorded (50 from individual-MT and 266 from coated-bead). Average peak force stayed relatively constant over the range of [ATP] used (Fig. 3.3) though forces got as high as 1.5 pN (Tables 3.1 & 3.2). The addition of ADP did not affect average peak force at an [ATP] of 0.5 mM (Fig. 3.4) and also reached forces as high as 1.5 pN (Tables 3.1 & 3.2). Corresponding average displacements, times to maximum displacement, and durations can be seen in Tables 3.1 and 3.2.

3.3 Discussion

Axonemal dynein, no matter what its subtype, is always in an array of other axonemal dyneins *in vivo*. How it functions individually and in groups is equally important as this reveals fundamental properties of the motor and how those properties can be coordinated with those of other nearby motors. With the individual-MT and coated-bead optical tweezers assays, we were able to observe two different setups as far as motor numbers. The coated-bead assay allowed for larger amounts of data to be taken where the orientation between dynein and the MT and the number of dynein motors interacting was much less limited. The individual-MT assay then made up for this lack of specificity and arranged for just a few dynein to interact with an individual MT.

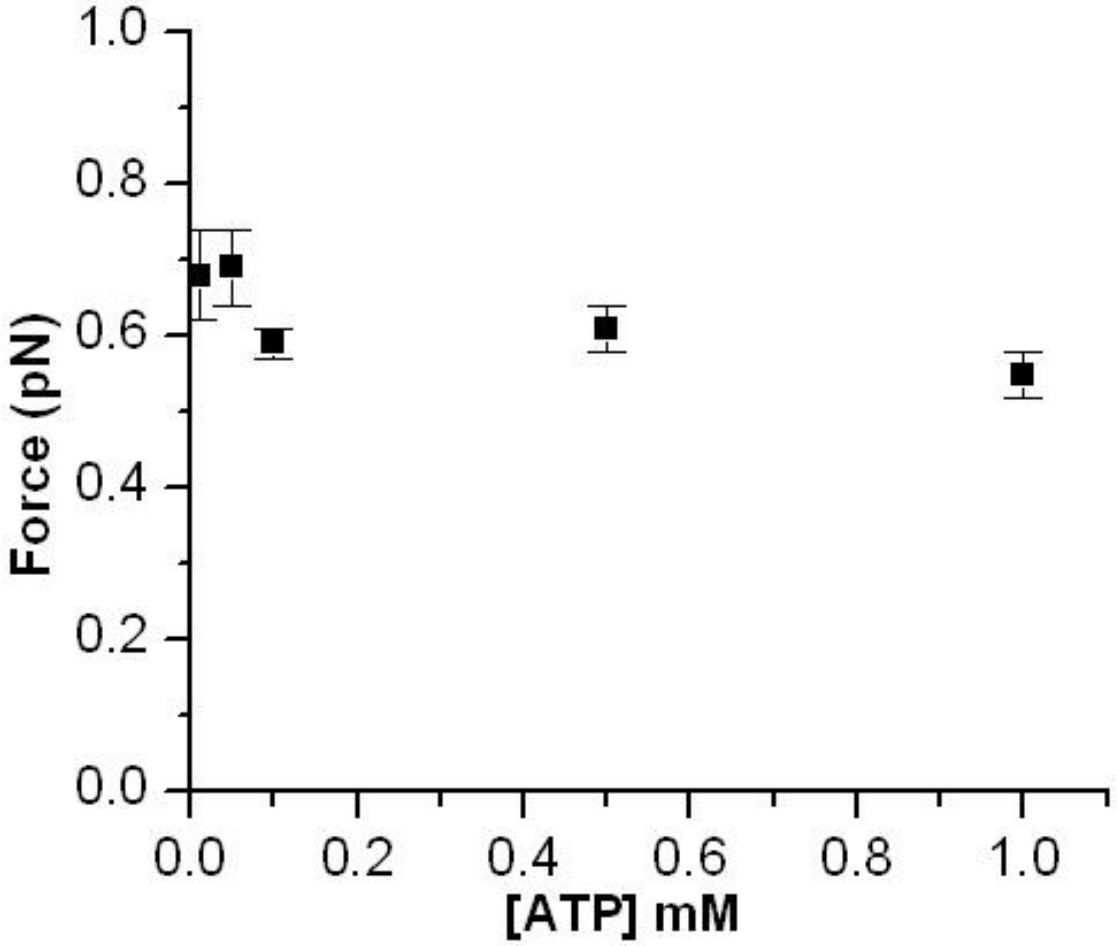

Figure 3.3: Average Dynein Peak Force ± SE Versus [ATP]

Average dynein peak force measured with optical tweezers for a range of [ATP] using the coated-bead assay with no ADP. An independent relationship between force and [ATP] was found. Each data point was calculated from 23 to 84 MT excursions.

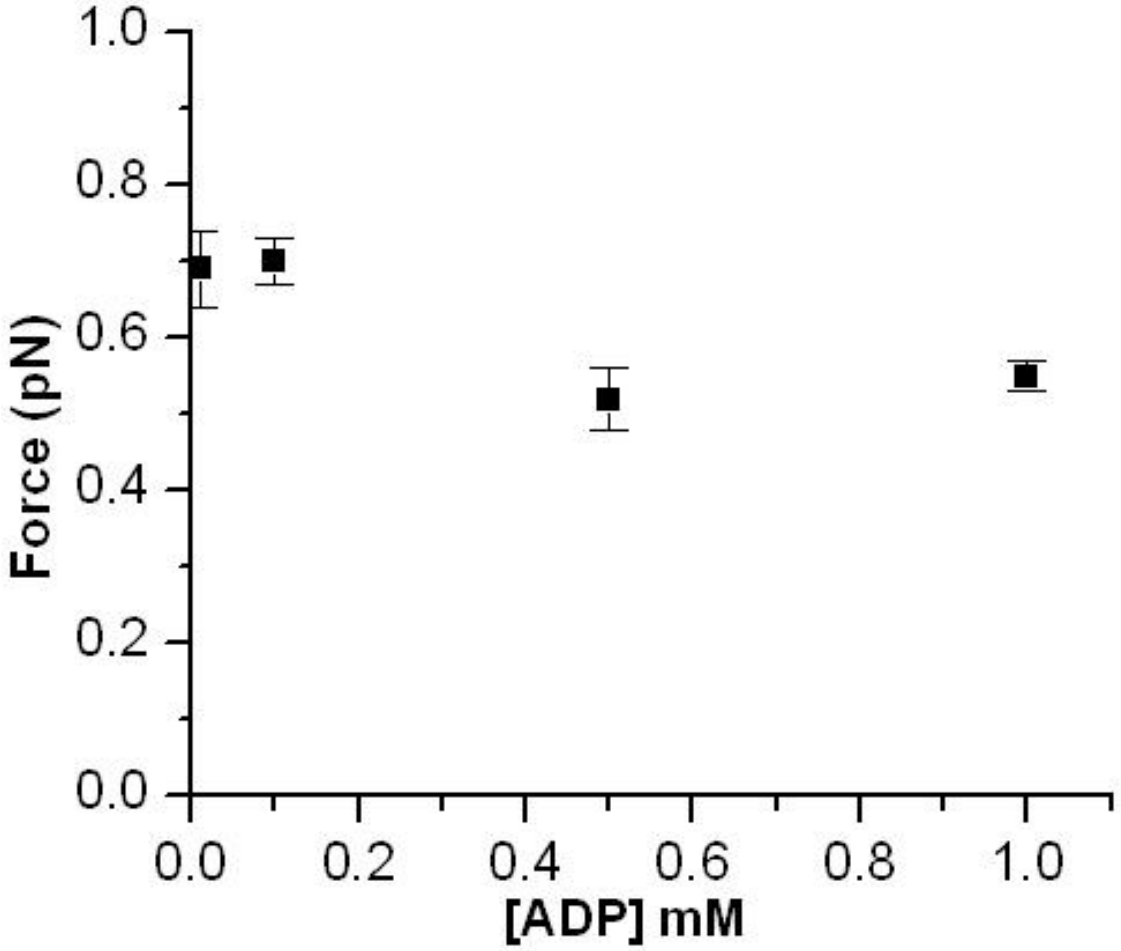

Figure 3.4: Average Dynein Peak Force ± SE Versus [ADP]

Average dynein peak force measured with optical tweezers for a range of [ADP] using the coated-bead assay with [ATP] = 0.05 mM. Each data point was calculated from 17 to 40 MT excursions.

Together, these observations made it possible to compare and contrast mammalian axonemal dynein in a loaded state in few to many motor numbers.

Previous work with cytoplasmic dynein have shown it to be processive [Cho et al., 2008; King and Schroer, 2000; Ross et al., 2006], in that it is able to move MTs long distances at low and high motor densities. In our gliding assay experiments with unloaded MTs, we found no relationship between velocity and MT length (motor number) though these were at motor numbers greater than ~49 which is still a fairly large amount [Lorch et al., 2008]. During the optical tweezers coated-bead assays, the geometry was similar to this except the MTs were now loaded, and the number of motors was fewer. The displacements of excursions caused by dynein were mostly short (< 100 nm) in length. Presumably, the longer displacements were from the rarer instances where a longer MT landed parallel to the dMT where many dyneins could all interact and transport it in larger motor numbers processively. These longer displacements have extremely low velocities even when [ATP] was relatively high expecting velocities in the range of microns/second (as seen from our gliding assay). The individual-MT experiments (where it is likely that 4 or fewer dyneins could have interacted with the MT at any one time) in particular then helped to clarify further what happens at more definite low motor numbers. The displacements were still short in length and the occurrences of the longer displacements were even rarer than with the coated-bead assay and still with slow velocities. These short stints in MT gliding, especially where motor numbers are low indicates that mammalian axonemal dynein individually is non-processive.

The question emerges as to whether axonemal dynein has a need to be processive. It is possible that processivity could have been lost from its evolution out of the cytoplasm [Mitchell, 2007] where processivity is crucial for being able to travel along MTs without releasing before its full trek and ending up at an unintended location. It does not seem that axonemal dynein would have this need inside of the axoneme since it is always in series with other motors, is geometrically constrained by the structure of the axoneme, and on an individual motor level does not need to move a dMT too far of a distance (about 300 nm for a full bend of the flagella). Also, processivity for axonemal dynein would mean it would produce consistent speeds no matter how many motors are interacting with the dMT. Different parts of the axoneme must be shearing at different speeds (for example the basal end would have a speed of zero) at any one time during a flagellar beat. It is not possible for the same number of dyneins to be pulling on a neighboring dMT at any one time seeing as the dMTs likely separate as the beat propagates [Aoyama and Kamiya, 2005] making different numbers of dyneins interact with the dMT at any one period of time.

The excursions in the individual-MT and coated-bead assays are most likely one or few single steps considering the short distances. The single step size that we found of 4.4 nm is reasonably consistent with kinesin [Block, 1995] within a factor of 2 and is the size of about 1 tubulin monomer. Though, this is a lower bound considering that the series compliance between the dynein, the MT, and the bead, prevents estimating the exact step size. Assuming step sizes on the order of 8 nm (1 tubulin dimer) and how fast a MT should be gliding based on the gliding assay (microns per second), the coated-bead

and individual-MT durations in time are actually fairly long. If dynein's binding and unbinding is related directly to the ATPase cycle, then it would be expected that these durations would be much shorter in time, on the order of milliseconds as opposed to what is seen on the order of 100s of milliseconds. This could indicate that a single round through dynein's ATPase cycle is not as simply correlated to an attachment, power-stroke, and release from its filament as is found for kinesin when under load. So why the wait? There have been some thoughts related to whether the stalk of the dynein motor is actually stiff enough for a protein conformational change at the head to translate to a difference at the MT binding site at the end of the stalk [Lindemann and Hunt, 2003]. Perhaps something other than the ATPase cycle at the head causes a change in the power-stroke cycle seeing as the dynein seems to be holding on for longer than would be expected from the ATPase cycle. In the optical tweezers assay, at the end of a single step, not much tension would be created and then dynein may not be able to unbind, causing longer durations. In the axoneme, other dynein would also be pulling, probably producing greater tension and making it easier for dynein to unbind. Dynein may not just be waiting for another ATP molecule to come along to unbind, but may actually need the tension and strain produced by other dynein pulling on the same MT in order to unbind.

Our measurements are the first direct mammalian dynein force measurements. While there haven't been forces measured for mammalian axonemal dynein, the range of forces for other systems/species have ranged greatly from around 1 pN [Mallik 2004] to tens of Piconewtons [Shingyoji 1998]. The Geometric Clutch Model [Schmitz et al., 2000] predicts that mammalian axonemal dynein would produce a force around 5 pN,

calculated from bending measurements relative to transverse forces between dMTs. The forces we measured were on the low end of this spectrum of forces. This could be due to several possibilities. The orientation of the dynein motors with respect to the MT may have put them into several different configurations where not as much force could be produced on the MT. With MTs coating the silica bead, they were not necessarily aligned along the dMT as dynein would naturally expect its neighboring MT to be. Dynein would then need to twist to pull on that MT. Some of the power stroke could be taken up in this re-orientation and/or may not be as stiff and not able to translate as much force. Also, there may have been drag produced on the MTs interacting with more than one dynein where some dynein were in a state of rigor not wanting to detach. This was seen in our gliding assays where frequently MTs would merely stay still along dMTs. Finally, it is possible that without ADP bound, the MT binding affinity was not as high as possible. This has been seen with mammalian axonemal dynein as the addition of ADP has caused increased bending in the flagella implying an increased force required to detach dynein from its neighboring dMT before allowing the flagella to bend in the opposite direction [Lesich et al., 2008]. With the excursions we observed likely being single or few steps and the behavior being non-processive, greater forces would only be expected to be developed when dynein is able to travel further and produce a higher peak force when working in high motor numbers. Considering these items, the forces we measured are likely then what an average, mammalian, axonemal dynein can produce individually.

For individual molecular motors in the kinesin and myosin families, force has been found to be independent of [ATP] [Finer et al., 1994; Meyhofer and Howard, 1995;

Svoboda and Block, 1994]. Cytoplasmic dynein has been hypothesized to act as if by a gearing mechanism increasing its force production and decreasing its step size with increases in [ATP] [Mallik et al., 2004]. This gearing relationship is not what we found with axonemal dynein, but more like kinesin and myosin as our observed forces stayed constant over similar ranges in [ATP]. While cytoplasmic dynein may have different cargoes that require different amounts of force in the same environment, axonemal dynein always has the same cargo. Axonemal dynein would have a need to produce different amounts of force depending on the cell's current needs since the flagella does have to alter its beat, but dynein may not have its force changed on the molecular level. It is also possible that different types of dynein along the dMTs can produce different forces over different distances and times based on [ATP]. In our optical tweezers assays, we could be accessing many of the types (7 types: 1 outer arm, 6 unique inner arms) of dynein (just as in our gliding assay) which could be averaging over those types and thus not finding a dependent relationship between force and [ATP]. Another possibility is that this consistency is indicative of accessing few to possibly only one motor at a time. The hydrolysis cycle could be the bottleneck producing a consistent force with each cycle hydrolyzing a single ATP. Force production may be independent of [ATP] because no matter what the concentration, if one cycle is correlated to one ATP molecule being hydrolyzed then this would produce the same protein reconfiguration and the same force produced each time.

We also found an independent relationship between observed forces and [ADP]. This is unexpected as ADP has caused an effect in many studies described earlier

(increasing MT translocation extent of sliding [Kinoshita et al., 1995b] and ATPase activity [Shiroguchi and Toyoshima, 2001]), including mammalian species [Lesich et al., 2008]. ADP's influence in the axoneme could get washed out by affecting only some of the dynein types. Or, for these dynein types it could be possible that the effect of ADP is only seen after incubation for long periods of time (10 minutes) as was seen with ADP increasing the acceleration of *Chlamydomonas* inner arm dynein 'a' [Kikushima et al., 2004]. With requirements in the optical tweezers assay to catch beads within minutes of addition before they settled to the point that it became too difficult to arrange the geometric setup, it is possible that ADP did not have enough time to have an effect on dynein's force production in our experiments.

These optical tweezers experiments have measured the force and displacements that mammalian dynein would make within the axoneme in 1 to few motor numbers. Excursions were generally short, but relatively long in duration compared to expectations of the ATPase cycle. We found from coated-bead and individual-MT optical tweezers assays that mammalian axonemal dynein on an individual motor level is non-processive, independent of [ATP] and [ADP] (at concentrations tested), and observed single step size. The axonemal system is a complicated one that is powered by a group of motors that have been tuned to work in that system. The more that is learned about how these molecular motors work individually and in groups, the more we will continue to understand how the axoneme works as a whole.

CHAPTER 4

DYNEIN'S MOTOR ACTIVITY & THE MAMMALIAN AXONEME

With the gliding assay and optical tweezers experiments completed, and data analyzed, several conclusions could be made concerning dynein's chemomechanical properties individually and in groups. These conclusions about velocity, processivity, step size, and force production based on [ATP] and [ADP] could then be used to answer questions (and ask new ones) concerning how dynein relates to the flagella's overall bending motion.

4.1 Conclusions & Implications for Mammalian Dynein & The Axoneme

From the gliding assay experiments, gliding velocity versus [ATP] was fit to a Michaelis-Menten model, giving expected velocities for how fast dynein can move unconstrained MTs. This model then made it possible to consider mammalian, axonemal dynein as an enzyme and compare its maximum velocity of 4.7 ± 0.2 μm/sec and K_m of 124 ± 11 μM to other dynein species. These values were consistent with axonemal dynein behavior observed in many mammalian [Bird et al., 1996] and non-mammalian [Kurimoto and Kamiya, 1991; Shiroguchi and Toyoshima, 2001; Yamada et al., 1998] systems. It was also found that translocation velocity was not dependent on the number of motors at motor numbers greater than about 49. More often than not, though, MTs would

just get stuck in place rather than glide. When there was gliding, it would glide for large distances.

When low motor numbers were tested, on the order of around 1 to 4 at a time, with the optical tweezers assays, the motors acted non-processively, moving for just short distances. Dynein working together can translocate for large distances, but when you get down to few or 1 dynein, they may only be able to take 1 or few steps at a time before releasing the MT. With these findings about how far and long a MT can be translocated by dynein in down to as few as 1 possible motor, the minimum step size could be estimated. This estimate is reasonably consistent with other molecular motors within a small factor of 2 and is the size of about 1 tubulin monomer. With these step size estimates and the finding that dynein actually seems to be holding onto the MT for a long period of time, it is possible that another factor in the cycle of binding and unbinding is required such as strain being necessary to unbind the MT. In the axoneme, other dyneins would also be pulling, probably producing greater tension and making it easier for dynein to unbind. This could have interesting implications for the ciliary/flagellar axoneme and dynein as a whole. As discussed before, there are several issues that come up with how dynein works and is regulated, either mechanically (such as using the Geometric Clutch Model) or chemically. One example of this is the question of how this flexible dynein protein can translate a conformational change at the head, along the stalk, and cause it to disconnect. from its MT substrate from the end of that stalk. It could be that strain is a major part of this process rather than just the ATPase cycle. The relatively long durations showing that strain may be necessary for MT release may provide a larger control over

the cycling of dynein's mechanical cycle than the hydrolysis of ATP. Also this is an indication that dynein may be regulated in a way by a requirement for strain to unbind, which fits well with the idea for GCM that dynein can be pulled from the MT with the force produced from the transverse force from flagellar bending.

Unlike with gliding velocity, an independent relationship between force and [ATP] was found. This indicates a difference in the effect of [ATP] at high and low motor numbers. As ATP concentration goes up, the more likely a motor would be in contact with a free ATP molecule to bind to, so the more often it would be active. For axonemal dynein, as a non-processive motor, the more motors that are translocating a MT, the faster it should go (up to a saturation point of maximum active dynein motors). It is expected then that on the 1 to few motor level that the force was measured at, velocity would also be independent of the [ATP] concentration. This independences from [ATP] on the level of an individual motor could be because no matter what the concentration of ATP, if one cycle is correlated to one ATP molecule being hydrolyzed then this would produce the same protein reconfiguration and the same force and velocity produced each time.

For both velocity and force, ADP did not produce increased activity upon its addition. Studies of the Geometric Clutch Model using whole flagella found that ADP did influence the force required to detach dynein and therefore did seem to regulate it. So why was this not seen in the gliding assay or optical tweezers studies done here? In the optical tweezers work, it is possible that few motors and types were accessed at any one

time causing the effect to not be seen. There was also the work with *Chlamydomonas* where ADP increased gliding acceleration [Kikushima et al., 2004]. This increase in activity needed minutes of incubation time with ADP. The optical tweezers studies may not have had incubation times long enough with attempts at speedily trying to get data before optical tweezers assay conditions with beads became more difficult. If this is not what is influencing the lack of increased activity, it could also be that certain types of dynein do have an increased influence on velocity and force from ADP in larger numbers.

It does not seem that axonemal dynein would have the need to be processive inside of the axoneme since it is always in series with other motors and on an individual motor level does not need to move a dMT too far of a distance (about 300 nm for a full bend of the flagella). Also, processivity for axonemal dynein would mean it would produce consistent speeds no matter how many motors are interacting with the dMT. Different parts of the axoneme must be shearing at different speeds at any one time during a flagellar beat. For example the basal end would have a speed of zero. It is not possible for the same number of dyneins to be pulling on a neighboring dMT at any one time seeing as the dMTs likely separate as the beat propagates making different numbers of dyneins interact with the dMT at any one period of time. The finding from these studies that dynein excursions were relatively short and velocities were different between few and many motors fits with these expectations about lack of processivity. At larger motor numbers, dynein can translocate a MT for large distances such as in our gliding assays, but at low motor numbers it does not seem to and also does not have a need to.

4.2 Future Directions

The main way that these studies could be improved is by increasing the control of the orientation of the MT attached to the bead in the optical tweezers trap relative to the dMT. As of right now, in the coated-bead assay, the orientation is not controlled at all, and in the individual-MT assay the MT must be draped across the dMT which puts it at an angle other than parallel (which that dMT's neighboring dMT would be physiologically inside of the axoneme). Some of the forces observed may have been low due to the fact that dynein was oriented in a fashion that it could not always be producing its full force on the MTs. This could possibly be done using multiple optical tweezers traps with a bead at either end of the MT. This would then allow the orientation of the MT to be controlled relative to the dMT. Though, if this is successful getting a MT consistently parallel to the dMT, these measurements would also be using higher motor numbers. To get individual motors translocating MTs in their more physiologic direction, other improvements would have to be made as will be described below.

If a way is found to isolate certain types of dynein in the mammalian axoneme while also keeping the motors connected in their proper place on the dMT, this would help get rid of the question of different types of dynein having different effects and possibly washing out the influence of other types. Currently it is not possible to remove mammalian, axonemal dynein from the dMT and still keep it functional which makes this a difficulty. Though even if this were possible, it would also have to be considered whether the dynein would be acting differently outside of its normal physiologic orientation connected to the dMT. If this isolation of dynein type on the dMT were done,

it would still raise the question of multiple motors versus individual motors talked about above. It would be another improvement on this method to also make it possible to lower the density of the dynein on the dMT to a point where it was certain that only an individual motor was being accessed while having the measuring MT still parallel to the dMT.

Finally, it would be beneficial to measure the forces necessary to unbind dynein from the MT by pulling on dynein stuck in rigor to a MT. This would be extremely difficult to perform due to not knowing if you are pulling with dynein actually actively pulling on the MT. A way to know in real time if an event is being produced by an active dynein while being sure that that active event is continuing would be needed. This would require a much more elaborate data acquisition software than was used in this work. As further processes and experimental designs are created and improved, these types of measurements should be possible.

REFERENCES

Aoyama S, Kamiya R. 2005. Cyclical interactions between two outer doublet microtubules in split flagellar axonemes. Biophysical Journal 89: 3261-3268.

Armstrong VL, Clulow J, Murdoch RN, Jones RC. 1994. Intracellular Signal-Transduction Mechanisms of Rat Epididymal Spermatozoa and Their Relationship to Motility and Metabolism. Molecular Reproduction and Development 38: 77-84.

Asai DJ, Koonce MF. 2001. The dynein heavy chain: structure, mechanics and evolution. Trends in Cell Biology 11: 196-202.

Avolio J, Glazzard AN, Holwill MEJ, Satir P. 1986. Structures Attached to Doublet Microtubules of Cilia - Computer Modeling of Thin-Section and Negative-Stain Stereo Images. Proceedings of the National Academy of Sciences of the United States of America 83: 4804-4808.

Bird Z, Hard R, Kanous KS, Lindemann CB. 1996. Interdoublet sliding in bovine spermatozoa: its relationship to flagellar motility and the action of inhibitory agents. J Struct Biol 116: 418-428.

Block SM. 1995. Nanometres and piconewtons: the macromolecular mechanics of kinesin. Trends in Cell Biology 5: 169-175.

Brokaw CJ. 1989. Direct Measurements of Sliding Between Outer Doublet Microtubules in Swimming Sperm Flagella. Science 243: 1593-1596.

Brouhard GJ, Schek HT, III, Hunt AJ. 2003. Advanced optical tweezers for the study of cellular and molecular biomechanics. IEEE Trans Biomed Eng 50: 121-125.

Burgess SA, Walker ML, Sakakibara H, Knight PJ, Oiwa K. 2003. Dynein structure and power stroke. Nature 421: 715-718.

Castoldi M, Popova AV. 2003. Purification of brain tubulin through two cycles of polymerization-depolymerization in a high-molarity buffer. Protein Expression and Purification 32: 83-88.

Chilvers MA, Rutman A, O'Callaghan C. 2003. Ciliary beat pattern is associated with specific ultrastructural defects in primary ciliary dyskinesia. Journal of Allergy and Clinical Immunology 112: 518-524.

Cho C, Reck-Peterson SL, Vale RD. 2008. Regulatory ATPase sites of cytoplasmic dynein affect processivity and force generation. Journal of Biological Chemistry 283: 25839-25845.

Clemmens J, Hess H, Lipscomb R, Hanein Y, Bohringer KF, Matzke CM, Bachand GD, Bunker BC, Vogel V. 2003. Mechanisms of microtubule guiding on microfabricated kinesin-coated surfaces: Chemical and topographic surface patterns. Langmuir 19: 10967-10974.

Finer JT, Simmons RM, Spudich JA. 1994. Single Myosin Molecule Mechanics - Piconewton Forces and Nanometer Steps. Nature 368: 113-119.

Gibbons IR, Rowe AJ. 1965. Dynein - A Protein with Adenosine Triphosphatase Activity from Cilia. Science 149: 424-426.

Goodenough UW, Heuser JE. 1985. Substructure of Inner Dynein Arms, Radial Spokes, and the Central Pair Projection Complex of Cilia and Flagella. Journal of Cell Biology 100: 2008-2018.

Hamasaki T, Holwill MEJ, Barkalow K, Satir P. 1995. Mechanochemical aspects of axonemal dynein activity studied by in vitro microtubule translocation. Biophysical Journal 69: 2569-2579.

Hess H, Clemmens J, Qin D, Howard J, Vogel V. 2001. Light-controlled molecular shuttles made from motor proteins carrying cargo on engineered surfaces. Nano Letters 1: 235-239.

Hirakawa E, Higuchi H, Toyoshima YY. 2000. Processive movement of single 22S dynein molecules occurs only at low ATP concentrations. Proceedings of the National Academy of Sciences of the United States of America 97: 2533-2537.

Hiratsuka Y, Tada T, Oiwa K, Kanayama T, Uyeda TQP. 2001. Controlling the direction of kinesin-driven microtubule movements along microlithographic tracks. Biophysical Journal 81: 1555-1561.

Ho HC, Granish KA, Suarez SS. 2002. Hyperactivated motility of bull sperm is triggered at the axoneme by Ca2+ and not cAMP. Developmental Biology 250: 208-217.

Hoff JD, Cheng LJ, Meyhofer E, Guo LJ, Hunt AJ. 2004. Nanoscale protein patterning by imprint lithography. Nano Letters 4: 853-857.

Howard J, Hudspeth AJ, Vale RD. 1989. Movement of Microtubules by Single Kinesin Molecules. Nature 342: 154-158.

Howard J, Hunt AJ, Baek S. 1993. Assay of microtubule movement driven by single kinesin molecules. Methods Cell Biol 39: 137-147.

Hunt AJ, Gittes F, Howard J. 1994. The force exerted by a single kinesin molecule against a viscous load. Biophys J 67: 766-781.

Hunt AJ, Howard J. 12-15-1993. Kinesin swivels to permit microtubule movement in any direction. Proc Natl Acad Sci U S A 90: 11653-11657.

Hyman A, Drechsel D, Kellogg D, Salser S, Sawin K, Steffen P, Wordeman L, Mitchison T. 1991. Preparation of Modified Tubulins. Methods in Enzymology 196: 478-485.

Kikushima K, Yagi T, Kamiya R. 2004. Slow ADP-dependent acceleration of microtubule translocation produced by an axonemal dynein. Febs Letters 563: 119-122.

King SJ, Schroer TA. 2000. Dynactin increases the processivity of the cytoplasmic dynein motor. Nature Cell Biology 2: 20-24.

Kinoshita S, Mikinoumura T, Omoto CK. 1995a. Regulatory Role of Nucleotides in Axonemal Function. Cell Motility and the Cytoskeleton 32: 46-54.

Kinoshita S, Mikinoumura T, Omoto CK. 1995b. Regulatory role of nucleotides in axonemal function. Cell Motility and the Cytoskeleton 32: 46-54.

Kurimoto E, Kamiya R. 1991. Microtubule Sliding in Flagellar Axonemes of Chlamydomonas-Mutants Missing Inner-Arm Or Outer-Arm Dynein - Velocity-Measurements on New Types of Mutants by An Improved Method. Cell Motility and the Cytoskeleton 19: 275-281.

Lesich KA, Pelle DW, Lindemann CB. 2008. Insights into the mechanism of ADP action on flagellar motility derived from studies on bull sperm. Biophysical Journal 95: 472-482.

Lindemann CB. 1994. A Geometric Clutch Hypothesis to Explain Oscillations of the Axoneme of Cilia and Flagella. Journal of Theoretical Biology 168: 175-189.

Lindemann CB. 2003. Structural-functional relationships of the dynein, spokes, and central-pair projections predicted from an analysis of the forces acting within a flagellum. Biophys J 84: 4115-4126.

Lindemann CB, Fentie I, Rikmenspoel R. 1980. A selective effect of Ni2+ on wave initiation in bull sperm flagella. J Cell Biol 87: 420-426.

Lindemann CB, Hunt AJ. 2003. Does axonemal dynein push, pull, or oscillate? Cell Motil Cytoskeleton 56: 237-244.

Lindemann CB, Schmitz KA. 2001. Detergent-extracted models for the study of cilia or flagella. Methods Mol Biol 161: 241-252.

Lorch DP, Lindemann CB, Hunt AJ. 2008. The motor activity of mammalian axonemal dynein studied in situ on doublet microtubules. Cell Motility and the Cytoskeleton 65: 487-494.

Mallik R, Carter BC, Lex SA, King SJ, Gross SP. 2004. Cytoplasmic dynein functions as a gear in response to load. Nature 427: 649-652.

Meyhofer E, Howard J. 1995. The Force Generated by A Single Kinesin Molecule Against An Elastic Load. Proceedings of the National Academy of Sciences of the United States of America 92: 574-578.

Mitchell DR. 2007. The evolution of eukaryotic cilia and flagella as motile and sensory organelles. 130-140.

Mocz G, Gibbons IR. 2001. Model for the motor component of dynein heavy chain based on homology to the AAA family of oligomeric ATPases. Structure 9: 93-103.

Moorjani SG, Jia L, Jackson TN, Hancock WO. 2003. Lithographically patterned channels spatially segregate kinesin motor activity and effectively guide microtubule movements. Nano Letters 3: 633-637.

Nicastro D, Schwartz C, Pierson J, Gaudette R, Porter ME, McIntosh JR. 2006. The molecular architecture of axonemes revealed by cryoelectron tomography. Science 313: 944-948.

Oiwa K, Sakakibara H. 2005. Recent progress in dynein structure and mechanism. Current Opinion in Cell Biology 17: 98-103.

Omoto CK, Yagi T, Kurimoto E, Kamiya R. 1996. Ability of paralyzed flagella mutants of Chlamydomonas to move. Cell Motility and the Cytoskeleton 33: 88-94.

Reuther C, Hajdo L, Tucker R, Kasprzak AA, Diez S. 2006. Biotemplated nanopatterning of planar surfaces with molecular motors. Nano Letters 6: 2177-2183.

Riveline D, Ott A, Julicher F, Winkelmann DA, Cardoso O, Lacapere JJ, Magnusdottir S, Viovy JL, Gorre-Talini L, Prost J. 1998. Acting on actin: the electric motility assay. European Biophysics Journal with Biophysics Letters 27: 403-408.

Ross JL, Wallace K, Shuman H, Goldman YE, Holzbaur ELF. 2006. Processive bidirectional motion of dynein-dynactin complexes in vitro. Nature Cell Biology 8: 562-570.

Sakakibara H, Kojima H, Sakai Y, Katayama E, Oiwa K. 1999. Inner-arm dynein c of Chlamydomonas flagella is a single-headed processive motor. Nature 400: 586-590.

Schmitz KA, Holcomb-Wygle DL, Oberski DJ, Lindemann CB. 2000. Measurement of the force produced by an intact bull sperm flagellum in isometric arrest and estimation of the dynein stall force. Biophys J 79: 468-478.

Sellers JR, Kachar B. 1990. Polarity and Velocity of Sliding Filaments - Control of Direction by Actin and of Speed by Myosin. Science 249: 406-408.

Shingyoji C, Higuchi H, Yoshimura M, Katayama E, Yanagida T. 1998. Dynein arms are oscillating force generators. Nature 393: 711-714.

Shiroguchi K, Toyoshima YY. 2001. Regulation of monomeric dynein activity by ATP and ADP concentrations. Cell Motility and the Cytoskeleton 49: 189-199.

Sugrue P, Avolio J, Satir P, Holwill MEJ. 1991. Computer Modeling of Tetrahymena Axonemes at Macromolecular Resolution - Interpretation of Electron-Micrographs. J Cell Sci 98: 5-16.

Sui HX, Downing KH. 2006. Molecular architecture of axonemal microtubule doublets revealed by cryo-electron tomography. Nature 442: 475-478.

Svoboda K, Block SM. 1994. Force and Velocity Measured for Single Kinesin Molecules. Cell 77: 773-784.

Uyeda TQP, Warrick HM, Kron SJ, Spudich JA. 1991. Quantized Velocities at Low Myosin Densities in An Invitro Motility Assay. Nature 352: 307-311.

Wang ZH, Khan S, Sheetz MP. 1995. Single cytoplasmic dynein molecule movements: Characterization and comparison with kinesin. Biophysical Journal 69: 2011-2023.

Weingarten MD, Suter MM, Littman DR, Kirschner MW. 1974. Properties of Depolymerization Products of Microtubules from Mammalian Brain. Biochemistry 13: 5529-5537.

Yagi T. 2000. ADP-dependent microtubule translocation by flagellar inner-arm dyneins. Cell Structure and Function 25: 263-267.

Yamada A, Yamaga T, Sakakibara H, Nakayama H, Oiwa K. 1-1-1998. Unidirectional movement of fluorescent microtubules on rows of dynein arms of disintegrated axonemes. J Cell Sci 111: 93-98.